Dynamics of Deoxyribonucleic Acid Solutions As Studied by Dielectric Relaxation Spectroscopy and Dynamic Mechanical Spectroscopy

Mingyun Sun,[†] Srdjan Pejanović,[‡] and Jovan Mijović*,[†]

Othmer Department of Chemical and Biological Sciences and Engineering, Polytechnic University, Six MetroTech Center, Brooklyn New York 11201, and Department of Chemical Engineering, Faculty of Technology, University of Belgrade, Belgrade 11000, Serbia & Montenegro

Received July 21, 2005; Revised Manuscript Received September 16, 2005

ABSTRACT: An investigation was carried out by dielectric relaxation spectroscopy (DRS) and dynamic mechanical spectroscopy (DMS) on the dynamics of aqueous solutions of deoxyribonucleic acid (DNA). Novel information is generated and presented through our use of wide temperature and frequency range in DRS and DMS measurements. Two relaxation processes were detected at temperatures below 273 K. The higher frequency, Debye-like process has an activation energy of 27 kJ/mol and is assigned to the bound water around DNA molecules. The lower frequency process is of the Cole−Cole type and has an activation energy of 55 kJ/mol, the same as that of pure ice. In the higher temperature range, encompassing the physiological condition, conductivity dominates the dielectric response. A pronounced peak in the dielectric modulus spectrum is observed, and its molecular origin is found to lie in the migration of counterions along the DNA surface. Using Manning's model, it was calculated that the subunit length over which counterions fluctuate increases from 70 nm at a concentration of 2 mg/mL to 153 nm at a concentration of 0.125 mg/mL. The results of DMS measurements of aqueous solutions of calf thymus DNA reveal a G'/G'' crossover point whose frequency (ω_C) scales with concentration as $\omega_C \sim C_{DNA}^{-2.4}$. The implication is that the DNA molecules behave as semiflexible polymers in aqueous solution. The temperature dependence of ω_C indicates that the breakup of the DNA base pairs and the chain melting begin at a temperature as low as 50 °C.

Introduction

Molecular dynamics of biomacromolecules, like synthetic polymers, cover a broad range of characteristic time and length scales, from very fast and localized, such as atomic fluctuations, to slow motions of the whole molecule, such as the globular to random coil transition in proteins. In all major types of biomacromolecules[1]—proteins, polysaccharides, nucleic acids, and lipids—the interplay of dynamics and structure governs their function in living organisms. Biomacromolecules are also often preserved by dry-freezing, and hence it is important to understand their dynamics in the range from low temperatures to the physiological conditions. Here we report on the dynamics of deoxyribonucleic acids (DNAs) in aqueous solution over a wide range of temperature and frequency.

DNA is composed of two strands: in the structure below "B" represents adenine (A), thymine (T), guanine (G), or cytosine (C).

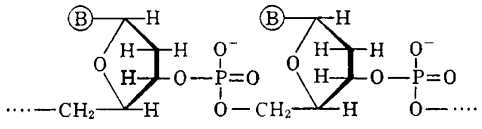

DNA takes up a double-helical conformation in its native state and a random coil conformation with separated strands in the denatured state. The DNA double helix is stabilized by hydrogen bonds between adenine and thymine (A−T) and between guanine and cytosine (G−C); A−T pairs have two and G−C pairs have three hydrogen bonds. Those base pairs can be separated by breaking the hydrogen bonds between them (using heat, pH value, or chemical agent such as urea or formamide) and transforming DNA from a double helix to a random coil. Melting takes place when the two strands open up during heating, and the melting point (T_m) of DNA is defined as the temperature at which 50% of the DNA has denatured, i.e., 50% of all base pairs (A−T and G−C) have opened up. The helix-to-coil transformation is favored by the electrostatic repulsion between the chains and the higher entropy of the coil. Some melted DNAs can reverse the denaturation process by slow cooling; this is called renaturation.

Outside the base pairs of DNA there are phosphate groups, carrying a net negative charge. When DNA is dissolved in an aqueous solution, some of the negative charge of the molecule is neutralized by cations, especially in saline solutions. This results in the formation of a counterion layer around the DNA molecules, called counterion sheath. The binding of counterions is nonlocalized, as proposed by Manning,[2] implying that the positive ions can move relatively freely along the DNA surface and within the surrounding hydration shell. According to Manning, the ions in an aqueous solution of DNA can be classified into three groups: condensed counterions, diffuse counterions, and bulk ions. Condensed counterions are hydrated but have a mobility to fluctuate along the DNA chain and are responsible for neutralizing some of the DNA charge. Diffuse counterions neutralize the rest of the charge, and their number density decreases exponentially with the distance from the DNA axis. Bulk ions are ions in the saline solution.

[†] Polytechnic University.
[‡] University of Belgrade.
* To whom correspondence should be addressed. E-mail: jmijovic@poly.edu.

10.1021/ma051596j CCC: $30.25
Published on Web 10/15/2005

The response of DNA molecule to an applied electrical field is of interest, but it remains incompletely understood. Unlike polypeptides, which have a permanent dipole moment in the peptide unit that is additive along the chain, the DNA double helix lacks a net permanent dipole moments due to the antiparallel direction of strands.[5] The dielectric response of DNA is believed to originate from an induced dipole moment due to the distortion of the counterion atmosphere by the applied electrical field[3,4] rather than the orientation of a permanent dipole moment. Early studies of dielectric properties of DNA[4] date back to the late 1940s, predating the Watson−Crick model.[6] Since then, with increasing knowledge of the structure and improving purification techniques, several dielectric studies of DNA have been conducted including experimental measurements[7−13] and molecular simulations.[14,15] Three relaxation processes in the aqueous solutions of DNA at room temperature have been reported;[16] the first is located in the low-frequency range below 1 kHz, the second is located in the frequency range between 1 MHz and 1 GHz, and the third is located above 1 GHz. These processes are termed α, β, and δ, respectively. The α process (which is not to be confused with the segmental α process in glass formers) is dependent on the DNA molecular weight, while the β process is not. Takashima[16] measured the dielectric permittivity for calf thymus and herring sperm DNAs in the frequency range from 20 Hz to 200 kHz and found that the dielectric permittivity of the α process decreases upon helix-to-coil transition. The α process has an asymmetric spectrum, with a steeper slope on the low-frequency side. The β process was observed between 1 MHz and 1 GHz by several investigators;[17−19] however, its origin remains unclear. Various explanations have been proposed, including bound water,[7] Maxwell−Wagner interfacial effects,[20] fluctuation of the counterion phase surrounding the DNA molecule,[21,22] redistribution of ions over limited segment lengths of the DNA chain,[23−25] and the hindered motion of base molecules.[4] The mechanism of the δ process is attributed to the bulk water in DNA solutions.

Reports of viscoelastic properties of DNA solutions measured by traditional rheometers are rare; one reason for that is the low viscosity of DNA solutions, and the other is the large amount of sample required. Mason et al.[26,27] have reported that linear viscoelastic behavior of DNA in solution has the markings of a semidilute polymer solution. Microrheology[27−35] offers a novel way to probe the dynamics of biological molecules at a single molecule level. Laser tweezers are used to manipulate dielectric probe microparticles (tracer) and investigate the rheological properties of the surrounding complex fluid. The motion of the tracer particles is tracked, and the mean-square displacement $\langle r^2 \rangle$ is calculated. The mean-square displacement of the tracer particles is then used to determine storage and loss modulus of the complex fluid in the frequency domain. This technique holds promise in biological applications due to the small sample size, the ability to probe local inhomogeneities in living cells, and the possibility to study viscoelasticity at higher frequencies.

The aim of the present work was to gain a deeper insight into the nature of DNA dynamics in aqueous solutions. Novel information is generated and presented through our use of wide temperature and frequency range in DRS and DMS measurements.

Experimental Section

Materials. Calf thymus DNA (D4522) and herring testes DNA (D6898) were obtained from Sigma Co. and were used without further purification. DNA solutions were made by dispersing DNA samples into pure deionized water and equilibrating overnight.

Techniques. *Dielectric Relaxation Spectroscopy* (*DRS*). Our facility combines commercial and custom-made instruments that include a Novocontrol α high-resolution dielectric analyzer (3 μHz−10 MHz) and Hewlett-Packard 4291B rf impedance analyzer (1 MHz−1.8 GHz). Both instruments are interfaced to computers and equipped with heating/cooling controls, including Novocontrol's Novocool system custom-modified for measurements at low and high frequency.

Dynamic Mechanical Spectroscopy (*DMS*). Experiments were conducted using a Rheometric Scientific's Advanced Rheometric Expansion System (ARES) rheometer. Strain values were adjusted in the linear viscoelastic range which was determined by measuring storage and loss modulus as a function of strain.

Ultraviolet (UV) Spectrophotometry. DNA concentrations were measured by UV spectrophotometry on a Biorad SmartSpec 3000 spectrophotometer (BioRad Laboratories, Hercules, CA). Optical density results at 260 nm were interpreted using 50 μg/mL as the standard concentration of a solution of double-stranded DNA with an optical density at 260 nm of 1 unit.

Gel Electrophoresis. Molecular weights of DNAs were determined by resolving DNA samples on a 1% Tris Borate-EDTA agarose gel using a Biorad Mini-Sub Cell GT electrophoresis apparatus (BioRad Laboratories, Hercules, CA). Lambda DNA cut with EcoRI and HinDIII was used as a sizing standard (Promega Corp., Madison, WI). Gels were stained with ethidium bromide solution at 0.5 μg/mL. Ethidium bromide fluorescence was visualized using a Chemi Doc system (BioRad Laboratories, Hercules, CA) and densitometry performed using the Quantity One software (BioRad Laboratories, Hercules, CA).

Results and Discussion

Dielectric Relaxation Spectroscopy (DRS). Aqueous solutions of DNA are highly conductive, and hence relaxation processes, if any, may be masked by high-conductivity or low-frequency dispersion (LFD) such as hopping of charge carriers.[36] In this study we employ several methodologies to investigate conductive DNA solutions, including performing measurements at low temperature and using dielectric modulus and conductivity representations to analyze the DRS spectra. We studied two types of DNA but have not observed significant difference in their dielectric response.

Low-Frequency (LF), Low-Temperature Response. Dielectric permittivity (part A) and loss (part B) of the aqueous solution of calf thymus DNA (2 mg/mL), measured at low frequency and low temperature, are shown in Figure 1. Two relaxation processes in the frequency domain are clearly discerned between 173 and 213 K. These two processes are well separated within this temperature range, and each process is gradually encroached by conductivity with increasing temperature (between 213 and 263 K), as shown in Figure 2. The solid lines in Figures 1 and 2 are fits to the Havriliak−Negami (HN) functional form.[37] The best result are obtained by setting the HN parameter $a = b = 1$ for the higher frequency process (HFP) and $b = 1$ for the lower frequency process (LFP). That reduces the HFP to a Debye-like process, and the LFP to a symmetrical Cole−Cole type.[38] The Debye-like process has an activation energy of 27 kJ/mol and is attributed to the bound water around DNA molecules. The calculated

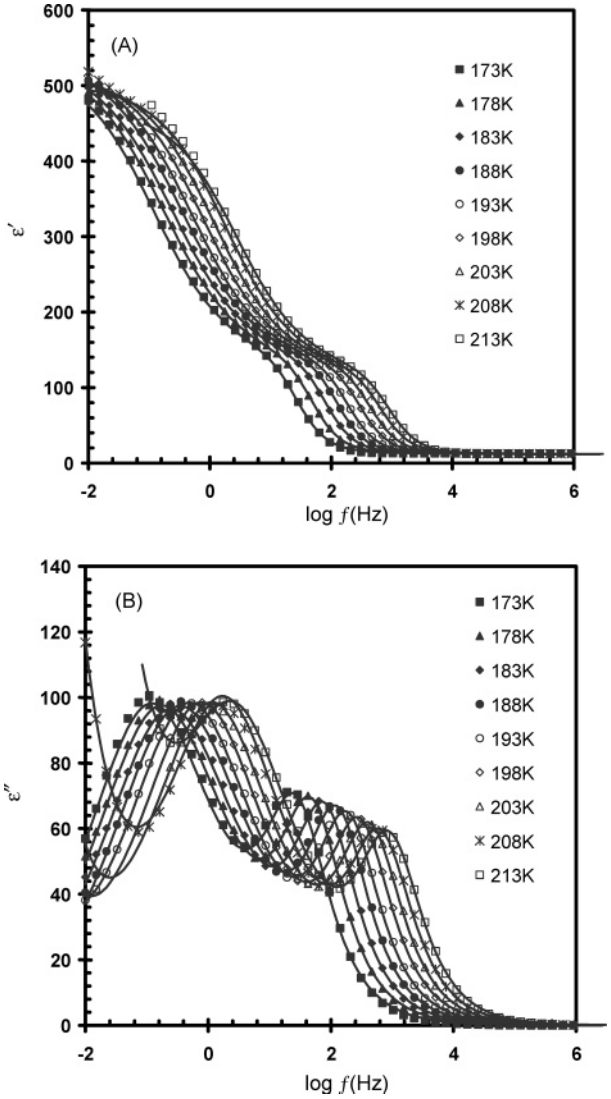

Figure 1. Dielectric permittivity (A) and loss (B) in the frequency domain for the aqueous solution of calf thymus DNA (2 mg/mL) with temperature as a parameter. Note: the temperature range is from 173 to 213 K.

activation energy is similar to that previously reported by Mashimo.[39]

The temperature dependence of the average relaxation time for HFP and LFP was examined next. The average relaxation time for each process was obtained from the HN fits, and the results are plotted in Figure 3. Both HFP and LFP obey the Arrhenius equation, with the activation energy shown in Figure 3. Also included in Figure 3 for comparison are the relaxation times for DNA solutions of different concentration. It is interesting to note that both HFP and LFP are independent of DNA concentration. The LFP has an activation energy of 55 kJ/mol, the same as that of pure ice.[40] Between 173 and 213 K, the relaxation time increases more slowly with decreasing temperature, showing the activation energy of 24 kJ/mol. Note also that pure deionized water follows the same trend as the DNA solutions within the same temperature range. This supports the tenet that the LFP originates from ice in the DNA−ice matrix.

We next turn our attention to the dielectric loss spectra with different DNA concentration. Figure 4 shows dielectric loss in the frequency domain for the aqueous solution of calf thymus DNA at 203 K, with

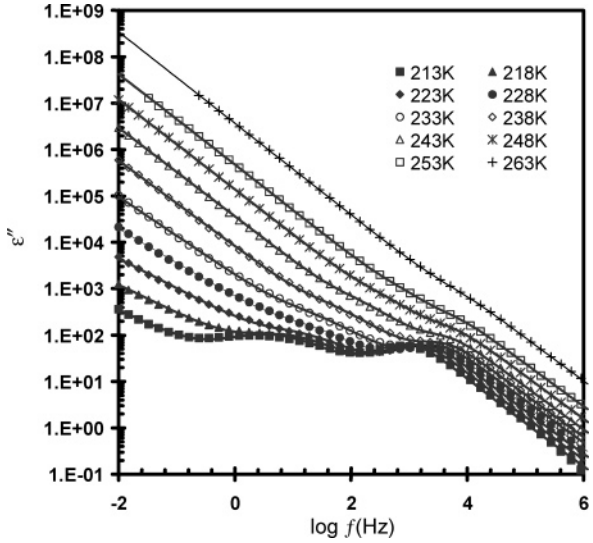

Figure 2. Dielectric loss in the frequency domain for the aqueous solution of calf thymus DNA (2 mg/mL) with temperature as a parameter. Note: the temperature range is from 213 to 263 K.

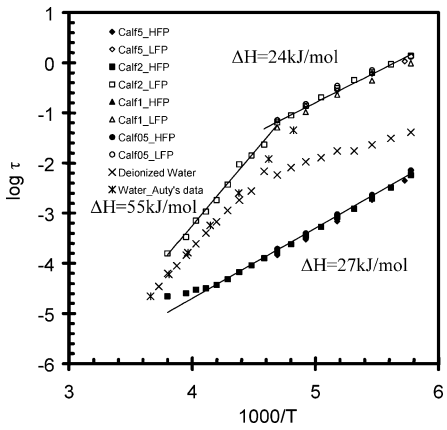

Figure 3. Temperature dependence of the average relaxation time for HFP (solid symbols) and LFP (open symbols) for the aqueous solution of calf thymus DNA solution (2 mg/mL) within temperature range from 183 to 263 K. Data for pure deionized water are included.

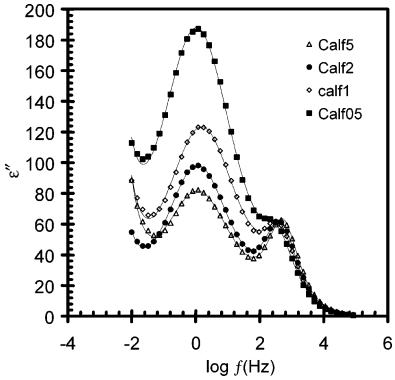

Figure 4. Dielectric loss in the frequency domain for the aqueous solution of calf thymus DNA at 203 K with DNA concentration (0.5−5 mg/mL) as a parameter.

DNA concentration as a parameter. The dilution of DNA significantly increases the dielectric strength of the LFP but decreases that of HFP. HN calculations following spectral deconvolution reveal that dielectric strength of LFP increases from 350 at 5 mg/mL to 847 at 0.5 mg/mL, and that of HFP decrease from 110 at 5 mg/mL to

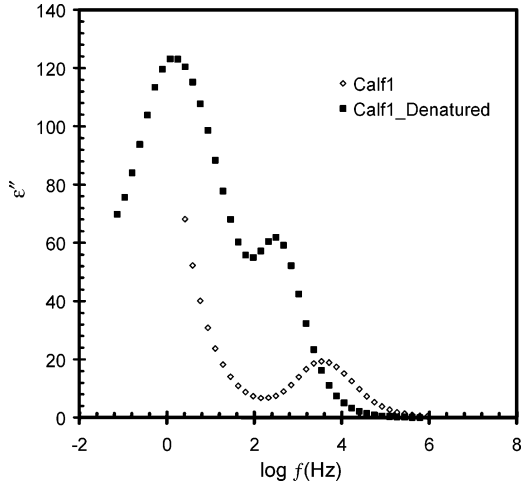

Figure 5. Dielectric loss in the frequency domain at 203 K for the aqueous solutions of calf thymus DNA (1 mg/mL) in its native and denatured state.

64 at 0.5 mg/mL. This is not surprising because the content of ice increases and that of bound water decreases with dilution of DNA solutions, causing the dielectric strength of LFP to decrease and that of HFP to increase. The relaxation rates of both LFP and HFP are independent of DNA concentration; i.e., the frequency of maximum loss (f_{max}) of each spectrum is independent of DNA concentration.

To probe the effect of molecular configuration on DNA dynamics, we compared two kinds of DNA solutions: (1) native double-helical configuration and (2) denatured, single-stranded random coil. The denatured DNA solutions were obtained by adding formamide (50 wt %) into the aqueous solution of the native calf thymus DNA. Formamide denatures the DNA by directly reacting with the bases, thereby disrupting normal base-pairing. The denatured DNA solution shows only one process at 203 K (see Figure 5), with a shorter relaxation time (higher frequency) than that of the bound water in the native DNA. Mashimo et al.[7] argued that bound water forms highly ordered clusters along and across the grooves of DNA, while the clusters are less ordered in the random coil state. The observed process in the denatured DNA solution may originate from the bound water around the separated strands of DNA. Because of the disordered alignment of water clusters around DNA coils, bound water would have more space to orient in response to the applied electrical field, thus speeding up the relaxation process in the denatured DNA.

An important question is how the type of solvent affects DNA dynamics? To that end we have also examined water/glycerol solutions of the herring testes DNA. The herring testes DNA was first dissolved in deionized water, and then glycerol was added to obtain a homogeneous solution. DRS spectra were generated for water/glycerol solutions of DNA, the solvent (glycerol plus deionized water), and pure glycerol, in the temperature range from 203 to 263 K. Figure 6 shows dielectric permittivity and loss for water/glycerol solution (0.27 wt %) of herring testes DNA in the frequency domain with temperature as a parameter. The dielectric spectra shift to lower frequency with decreasing temperature, and the solid lines in Figure 6 are the HN best fits. The average relaxation times obtained from the HN fits for pure glycerol, water/glycerol solvent, and DNA solution are plotted in Figure 7. The average

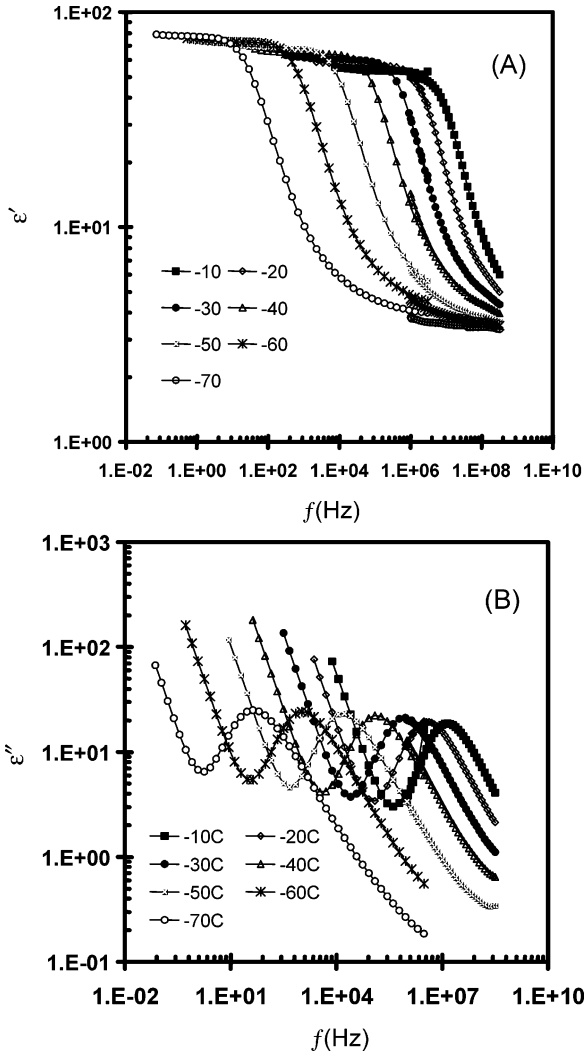

Figure 6. Dielectric permittivity (A) and loss (B) for the water/glycerol solution (0.27 wt %) of herring testes DNA in the frequency domain with temperature as a parameter.

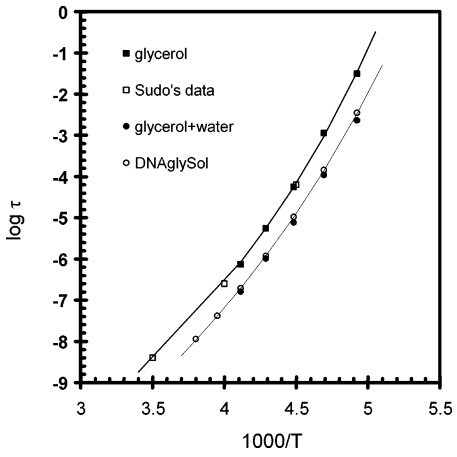

Figure 7. Temperature dependence of the average relaxation time for the water/glycerol solution of herring testes DNA, water/glycerol solvent, and pure glycerol.

relaxation time of pure glycerol is in agreement with Sudo et al.,[41] whose data are included in Figure 7 for comparison. The solid lines in Figure 7 are best fits to the Vogel−Fulcher−Tammann (VFT) function.[61] Pure glycerol and the water/glycerol mixture have parallel VFT-type temperature dependence. The addition of deionized water speeds up the relaxation process of

glycerol. Little difference is observed between the water/glycerol solvent and the water/glycerol solution of DNA. It is interesting to note that the aqueous solutions of DNA show similar dielectric behavior to pure water, with the same activation energy, while the water/glycerol solutions of DNA show similar dielectric behavior to pure glycerol, with a parallel VFT curvature and a faster relaxation rate. The implication is that the dynamics of DNA solutions are dominated by the solvent. Interestingly, this is in agreement with Caliskan et al.,[42] who report that the temperature dependence of the quasi-elastic scattering (QES) intensity of Raman spectra in a protein solution (protein + solvent) and in the pure solvent (glycerol or trehalose) is the same. They conclude that the protein dynamics are controlled by the solvent dynamics even on the picosecond scale.

High-Frequency (HF), High-Temperature Response. A. Dielectric Spectra Representation. Dielectric spectra of polymers are generally represented using the permittivity formalism; however, it is not always easy to identify dielectric loss peaks for highly charged materials such as polyelectrolyte or DNA. In such a situation, dielectric modulus[43] and/or conductivity[44] spectra are employed as the preferred representation of data. For example, when both real and imaginary parts of dielectric permittivity are large, it is not advisable to use the permittivity format since relaxation processes, if any, may be masked by the low-frequency dispersions (LFD).[45] The masked relaxation process may be distinguished from the LFD by employing the complex dielectric modulus format.[45] Dielectric modulus is the reciprocal of complex permittivity and is expressed as

$$M^*(\omega) = M'(\omega) + iM''(\omega) = \frac{1}{\epsilon^*(\omega)} = \frac{\epsilon'(\omega) + i\epsilon''(\omega)}{[\epsilon'(\omega)]^2 + [\epsilon''(\omega)]^2} \quad (1)$$

The permittivity and the modulus formalisms contain information from the same measurement; however, they differ in the manner in which the underlying dielectric phenomena are highlighted or suppressed.[45] For example, $M''(f)$ plots may suppress LFD, which is significant in the $\epsilon''(f)$ plots. The peak masked by LFD in the permittivity presentation shows up in the modulus presentation, confirming the existence of a "hidden" process.[45] Besides, the conductivity in the $\epsilon''(f)$ plots shows a linear increase at low frequencies with $\epsilon''(f) \propto f^{-1}$; however, it appears as a pronounced Debye peak in the $M''(f)$ plots.[46] The calculated characteristic time from the peak value of $M''(f)$ is often referred to as conductivity relaxation time.[47] For a clearly discernible relaxation process in $\epsilon''(f)$ plots, the modulus spectrum shifts to higher frequency compared to that of the permittivity spectrum, by a factor related to the ratio of high- and low-frequency limiting permittivity. This factor is $\epsilon_\infty/\epsilon_0$ (as $\tau_M = (\epsilon_\infty/\epsilon_0)\tau_\epsilon$) for a single relaxation process (Debye process), and it becomes more complicated for a non-Debye process due to the distribution of relaxation times. The modulus formalism is widely used for analyzing data of ionically conducting glasses and melts.[48−51] Richert and Wagner[46] described how dielectric experiments can be conducted in two ways: (1) the constant field case, $E(t) = E_0$ for $t \geq 0$; (2) the constant charge case, $D(t) = D_0$ for $t \geq 0$, corresponding to dielectric retardation (ϵ) and relaxation (M), respectively. They measured the modulus in the time domain and found no discrepancy between the relaxation times calculated from the measured $M(t)$ data and the $\epsilon(f)$ data obtained from the impedance analysis.

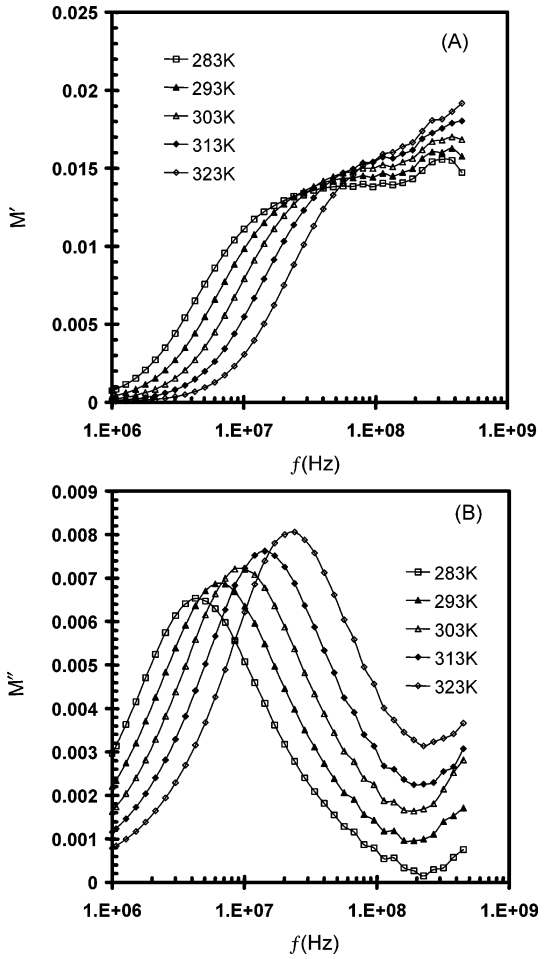

Figure 8. Dielectric modulus (A, real part; B, loss part) in the frequency domain for the aqueous solution of herring testes DNA (2 mg/mL) with temperature as a parameter.

Conductivity spectra offer another way to present data for ionically conducting systems. At low frequencies, $\sigma'(\omega)$ is constant at the dc value, $\sigma_0(T)$, which increases only with increasing temperature. At higher frequencies, however, the conductivity increases according to a power law $\sigma'(\omega) \sim \omega^p$ $(0 < p \leq 1)$. The best way to present dielectric spectra for ionically conducting systems is still the subject of debate. Moynihan[49−51] and co-workers employed modulus and conductivity formalisms and expressed a preference for the use of modulus because it behaves phenomenologically like a relaxation function. However, Parthun and Johari reported[52] that the permittivity formalism was more reliable than the modulus and impedance formalisms, based on their results for a solid electrolytes with both high dc conductivity and electrode polarization effects. Here we present our data using different formalisms for comparative purposes.

B. Temperature Dependence. Measurements were conducted on the aqueous solutions of herring testes DNA between 1 MHz and 1 GHz, in the temperature range from 283 to 323 K where DNA remains in its native state and the evaporation of water is negligible. Dielectric loss spectra show no peaks above 1 MHz. Real and imaginary components of the dielectric modulus for a 2 mg/mL solution are shown in Figure 8. Note how

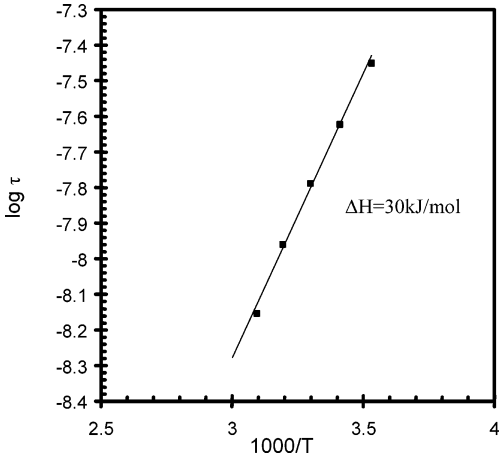

Figure 9. Temperature dependence of the average characteristic time for the aqueous solution of herring testes DNA (2 mg/mL) within temperature range from 283 to 323 K.

the loss modulus peak shifts systematically with temperature. The solid lines in Figure 8A,B are fits to the modified HN functional form:

$$M^*(\omega) - M_0 = \frac{\Delta M}{[1 + (i\omega\tau_M)^a]^b} \quad (2)$$

The average characteristic time (τ_M) from the HN equation is very close to that calculated from the data using $\tau = 1/2\pi f_{max}$. The temperature dependence of the average characteristic time (τ_M) is of the Arrhenius form, and the calculated activation energy is 30 kJ/mol, as shown in Figure 9. It is sometimes difficult to tell the Vogel−Fulcher−Tammann (VFT) from the Arrhenius temperature dependence in a narrow temperature range. In such cases Mozine suggests[45] the use of the following equation to distinguish between those two forms:

$$\left[\frac{d \ln \tau}{d(1/T)}\right]^{-1/2} = \frac{1}{\sqrt{B}} - \frac{T_0}{\sqrt{B}} \times \frac{1}{T} \quad (3)$$

where all parameters are as defined in the VFT equation. If the plot of the derivative of ln(τ) against the inverse of temperature ($1/T$) shows that ln(τ) is independent of temperature, then $T_0 = 0$ and the VFT equation reduces to the Arrhenius equation. The Arrhenius form of the characteristic time (τ_M) has been verified by eq 3.

The dielectric modulus strength, defined as $\Delta M = M_\infty - M_0$, is proportional to dielectric strength ($\Delta\epsilon$) and was calculated using $M_0 = 1/\epsilon_0$ and $M_\infty = 1/\epsilon_\infty$.[53] ΔM for the observed process (Figure 8) increases with increasing temperature, and the value obtained from the HN fits is shown in Figure 10. The resulting spectrum is nearly Debye-like, and the HN parameters a and b are within the range 0.95−1.

Conductivity spectra in the frequency domain are shown in Figure 11 for a 0.25 mg/mL aqueous solution of herring testes DNA. Analogous results were observed for other concentrations; however, the transition from the dc to the frequency-dependent conductivity shifts to higher frequency with increasing concentration. Figure 11 represents a typical conductivity plot for an ionically conductive system. At low frequencies, $\sigma'(\omega)$ is constant at the dc value $\sigma_0(T)$. $\sigma'(\omega)$ increases at high frequencies according to a power law $\sigma'(\omega) \sim \omega^p$. $\sigma_0(T)$ increases with increasing temperature, but the frequency that marks the onset of the transition from the dc to the frequency-dependent conductivity is not a function of temperature. The slope of the frequency-dependent conductivity is nearly 2, and it decreases with increasing temperature from 1.94 at 283 K to 1.86 at 313 K.

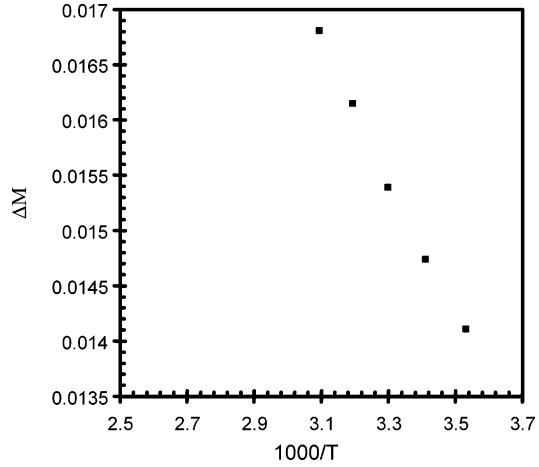

Figure 10. Dielectric modulus strength (ΔM) as a function of reciprocal temperature for the aqueous solution of herring testes DNA (2 mg/mL) within temperature range from 283 to 323 K.

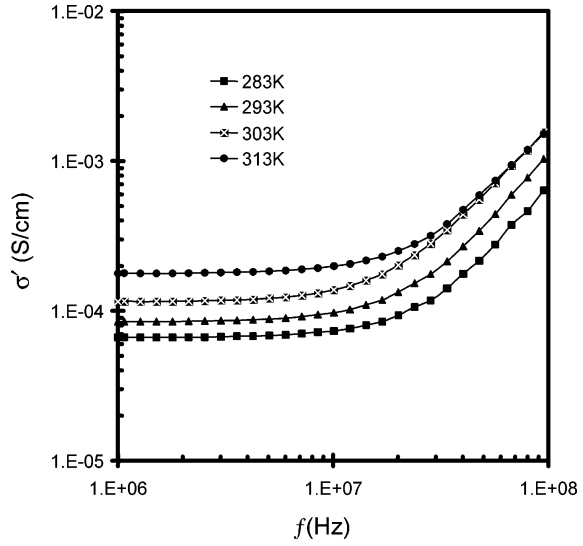

Figure 11. Conductivity in the frequency domain with temperature as a parameter for the aqueous solution of herring testes DNA (0.25 mg/mL).

C. Concentration Dependence. We next examine the concentration dependence of the dielectric modulus of DNA in its native state. Figure 12 shows dielectric modulus in the frequency domain with concentration as a parameter measured at 303 K. An increase in the DNA concentration speeds up the process as the peak shifts to higher frequency. The calculated average characteristic time (τ_M) and specific dielectric modulus strength ($\Delta M/c$) as a function of DNA concentration (mg/mL) are shown in Figures 13 and 14, respectively. The observed decrease in τ_M is in agreement with the previously reported result.[24,25] We note, however, that a weak β process ($\Delta\epsilon \sim 5$[24,25,54]) was not observed in our experiments.

Bone et al.[24] found that the average relaxation time (τ) decreases and dielectric strength ($\Delta\epsilon$) increases with increasing DNA concentration. This parallels our find-

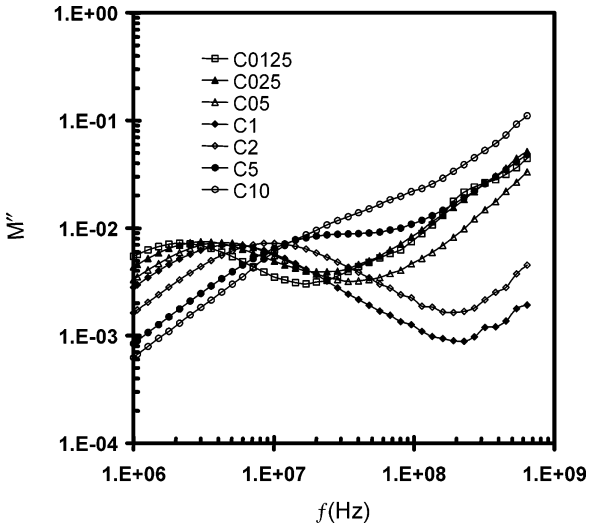

Figure 12. Dielectric loss modulus in the frequency domain measured at 303 K for the aqueous solution of herring testes DNA with concentration as a parameter.

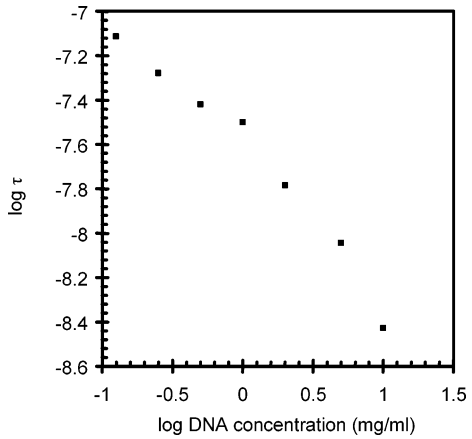

Figure 13. Concentration dependence of the average characteristic time for the aqueous solution of herring testes DNA.

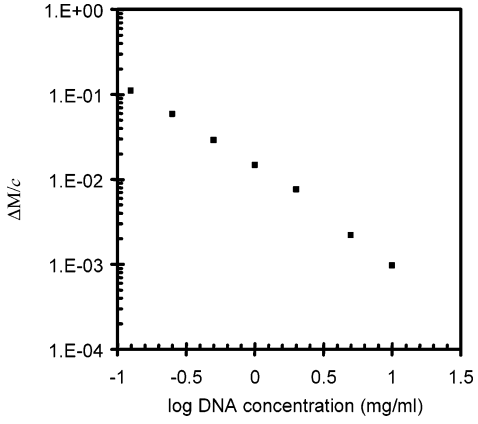

Figure 14. Concentration dependence of the specific dielectric modulus strength for the aqueous solution of herring testes DNA.

ing that the characteristic time (τ_M) decreases and dielectric modulus strength (ΔM) increases with increasing DNA concentration. Bone et al.[25] also observed that the specific dielectric strength ($\Delta\epsilon/c$) rises exponentially with decreasing DNA concentration for the aqueous solution of herring testes DNA. This too is in agreement with our results in that $\Delta M/c$ increases exponentially with decreasing DNA concentration, as

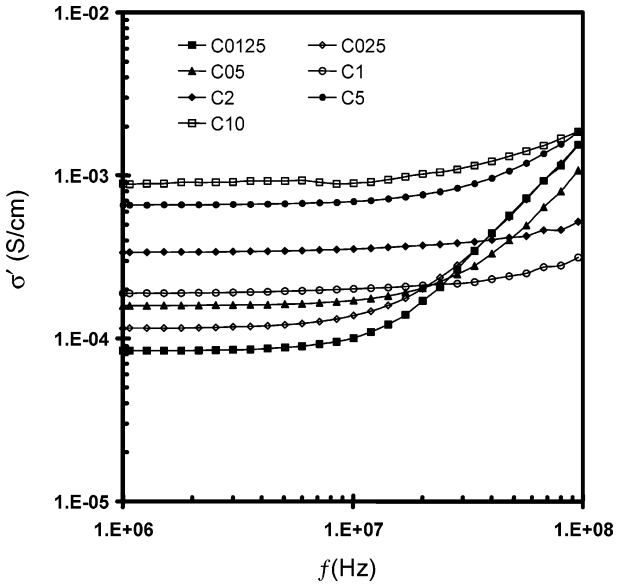

Figure 15. Conductivity in the frequency domain with DNA concentration as a parameter for herring testes DNA solutions.

shown in Figure 14. Note, however, that a different result was observed for small globular proteins that possess a permanent dipole moment. For example, South and Grant[55] studied whale myoglobin and observed a linear dependence of dielectric strength on concentration up to 180 mg/mL. For globular protein, the specific dielectric strength ($\Delta\epsilon/c$) is a characteristic parameter that is proportional to the square of the molecular dipole moment. But in the case of DNA the dielectric response stems from conductivity and counterion fluctuations along the DNA surface, not from the permanent dipole moment. Another factor may be due to the high number density of ions around DNA; the counterions have nonnegligible interactions with each other, i.e., the motions of counterions may no longer be independent of each other.

The concentration dependence of conductivity is shown in Figure 15. $\sigma_0(T)$ increases with increasing concentration, and the transition from the dc to the frequency-dependent conductivity shifts to higher frequency with increasing concentration. The slope decreases with increasing concentration, and it is difficult to obtain physically meaningful fits of data to the power law form $\sigma'(\omega) \sim \omega^p$ above 1 mg/mL.

D. Origin of the Dielectric Response—Counterion Fluctuations. We next address the question of the origin of the dielectric response observed in the high frequency/high temperature range. It is generally believed that the dielectric dispersions in DNA solutions may be attributed to the counterion polarization, although the precise molecular origin of those processes is not fully understood. Takashima,[4] Mandel,[18] and Touw and Mandel[56] studied α and β processes and argued that both relaxations originate from the motions of ions around the DNA molecules. The α process is due to the migration of counterions along the whole DNA chain and as such depends on the molecular weight, while the β process, located in the megahertz range at room temperature, arises from the migration of counterions over a segment of DNA chain and is independent of molecular weight.

DNA conformation affects dielectric dispersion. Initially, it was argued that a highly charged rigid-rod macromolecule, such as synthetic polyelectrolyte, charged

polypeptides, or DNA, should show one dielectric dispersion, whose characteristic time is related to the distribution of counterions along the whole rod.[56,57] However, this concept was not corroborated by experimental results. The model of DNA as a rigid rod was then modified into a wormlike chain made of a sequence of mechanically rigid subunits connected at a fixed angle. Counterions condense around the DNA and are freely redistributed within a limited subunit length, giving rise to the higher frequency dispersion (the β process). Manning[58] determined a critical factor, ξ, proportional to the DNA molecular charge density, which determines whether the counterion condensation process can occur. ξ can be calculated from

$$\xi = \frac{q^2}{4\pi\epsilon_0\epsilon_r kTb} \tag{4}$$

where q is the electronic charge, ϵ_r is the dielectric permittivity (real part) of the solvent, and b is the average distance between charged sites. The condition for condensation is $\xi \geq 1/z$, where z is the valence of the counterion. For a DNA double helix in aqueous solution, the calculated value of ξ is 4.17[24] ($b = 1.7$ Å between phosphate pairs), and counterion condensation is predicted. Then the fraction of condensed counterions is given by $\phi = 1 - z^{-1}\xi^{-1}$, and the value of ϕ for monovalent ions is 0.76. Manning[58] derived the expression for the polarizability of the condensed counterion layer along a direction parallel to the DNA axis and obtained the predicted relaxation time (τ) and dielectric strength ($\Delta\epsilon$) for the counterion fluctuation process within a subunit length L_s as

$$\tau = \frac{{L_s}^2 Aq}{\pi^2 kT\mu} \tag{5}$$

$$\frac{\Delta\epsilon}{c} = \frac{z^2q^2nA{L_s}^2}{36\epsilon_0 kT} \tag{6}$$

where L_s is the subunit length over which ions can fluctuate freely for redistribution in response to the external electrical field and factor A accounts for the dependence of the stability of the ionic phase on the electrolyte concentration according to

$$A = \frac{1}{1 - 2(z\xi - 1)\ln(\kappa b)} \tag{7}$$

where b is the average distance between charged sites and κ is the Debye screening parameter given by[59]

$$\kappa = \left[4\pi N_A\left(\frac{q^2}{4\pi\epsilon_0\epsilon_r kT}\right)\left[C_i z^2 + \left(\frac{1}{\xi}\right)C_p\right]\right]^{0.5} \tag{8}$$

where N_A is the Avogadro's number; C_i and C_p are the molar concentrations of ions in the buffer and phosphate groups, respectively. In eqs 4 and 5, q is the electronic charge, ϵ_0 the permittivity of vacuum, kT the thermal energy, μ the counterion mobility, z the valence of the ion, n the number of condensed counterions given as $n = \phi L_s/zb$, and c the number density of subunits which can be written as $c = N_A C_p(b/L_s)$.

Our experimental data can be explained by Manning's model, suggesting that the observed dielectric process represents conductivity due to the migration of counterions along the DNA surface. A detailed picture of the underlying physics that emerges from our study is as follows. Consider the temperature dependence and the DNA concentration dependence of the dielectric modulus strength and the characteristic time calculated from the modulus spectra. The decrease in the specific dielectric increment ($\Delta M/c \propto \Delta\epsilon/c$) with increasing DNA concentration (Figure 14) reflects an increase in the subunit length and a more stretched conformation in dilute DNA solutions. This trend can be also surmised from the decrease in the characteristic time with increasing DNA concentration (Figure 13), which is in agreement with previous reports.[24,25,54] We can estimate the ion mobility by calculating the ratio of the specific dielectric increment and the characteristic time; the result shows that the ion mobility decreases with increasing DNA concentration and levels off at 5 mg/mL. If we consider DNA solutions as dilute at a concentration below 2 mg/mL, the calculated subunit length (ion mobility of Na^+ in dilute solutions is $\mu = 5 \times 10^{-8}$ m^2/(V s)[5]) increases from 70 nm at concentration of 2 mg/mL to 153 nm at concentration of 0.125 mg/mL. The increase in the subunit length of DNA indicates that counterions migrate over a longer distance and that the conformation of DNA becomes more rigid upon dilution.

The temperature dependence of the dielectric modulus strength (ΔM) is considered next. The motions of counterions are thermally activated, resulting in a longer subunit length. At a constant DNA concentration, ΔM increases with increasing temperature (Figure 10), indicating that ${L_s}^2/T$ (eq 5) also increases with increasing temperature. By plotting $T\Delta M$ as a function of temperature, we find that $T\Delta M$ increases with increasing temperature. Since A (eq 7) is only a weak function of temperature,[58] it follows that the subunit length increases with increasing temperature as the consequence of a thermally activated process. The decrease in the characteristic time suggests that the increase in ion mobility is greater than the increase in ${L_s}^2/T$ with increasing temperature. The ratio of the specific dielectric strength and the characteristic time shows that the ion mobility increases faster than the subunit length with increasing temperature.

E. Chain Melting Effect. To obtain single-stranded denatured DNA, aqueous solutions were heated to 95 °C for 10 min, quenched into an ice−water mixture, and subsequently tested. We found that the magnitude of dielectric permittivity and loss were consistently higher in the denatured DNA solutions, as shown for several DNA concentrations in Figure 16. This finding is in agreement with the results reported by Baker-Jarvis et al.[3] and Georgakilas.[60] The higher conductivity in a single-stranded DNA solution is at least in part due to the increased number of counterions released upon the separation of strands. This is in further agreement with the reported[60] stages of DNA denaturation process, whereby in the first stage the counterions are expelled from the molecules, causing stronger phosphate−phosphate repulsions that separate the strands.

Dynamic Mechanical Spectroscopy (DMS). We next present the results of DMS measurements of the linear viscoelastic storage (G') and loss (G'') modulus in the frequency domain for aqueous solutions of DNA. The average molecular weights of DNAs determined by gel electrophoresis were 2163 and 989 kg/mol for the calf thymus DNA and the herring testes DNA, respectively. The viscosity of aqueous solutions of calf thymus

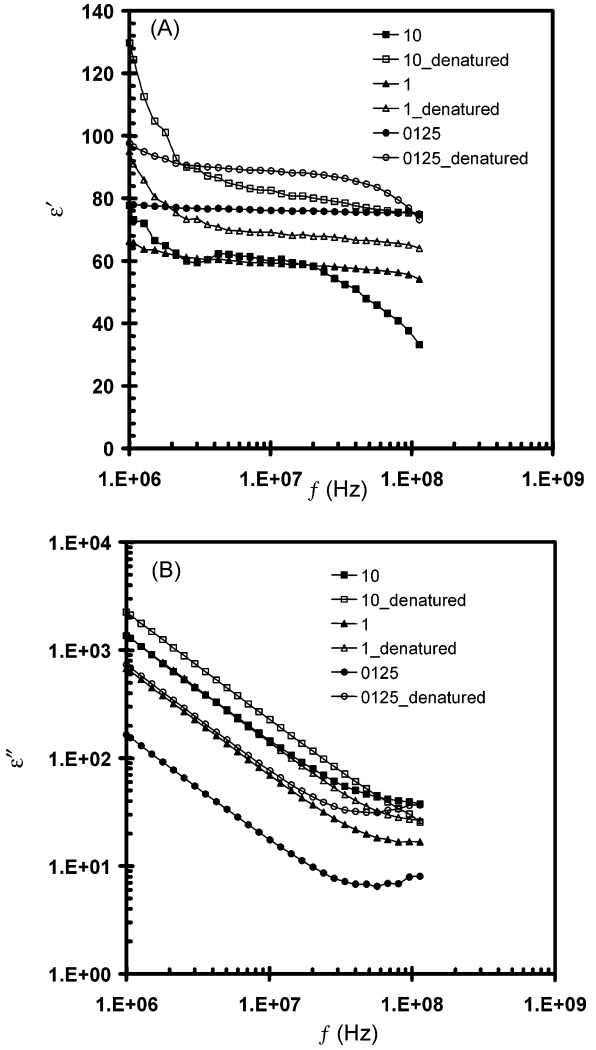

Figure 16. Dielectric permittivity (A) and loss (B) in the frequency domain measured at 303 K for the native and thermally denatured aqueous solution of herring testes DNA with concentration as a parameter.

DNA increases with increasing DNA concentration; however, the viscosity of aqueous solutions of herring testes DNA varies little with increasing DNA concentration. Because of the minimum required torque, DMS measurements were conducted only on the DNA solutions with sufficiently high viscosity. Aqueous solutions of calf thymus DNA could be measured above the concentration of 1 mg/mL, but those of herring testes DNA could not be measured even above the concentration of 10 mg/mL. The linear viscoelastic range was determined by measuring G' and G'' as a function of strain. For strains below 70%, G' and G'' are independent of the shear rate $\dot{\gamma}$. We choose the strain of 50% (at this value the calf thymus DNA solutions are measurable with our ARES instrument and are within the linear viscoelastic range). The evaporation during measurements was minimized by a Teflon enclosure placed around the samples. Storage and loss modulus in the frequency domain with DNA concentration as a parameter are shown in Figure 17. G' and G'' exhibit a crossover at a crossover frequency (ω_C), and they scale with power laws of $G' \propto \omega^{0.8}$ and $G'' \propto \omega^{0.5}$. The crossover frequency shifts to lower frequency with increasing DNA concentration, as the motions of DNA molecules become impeded. The scaling power of ω_C vs DNA concentration is $\omega_C \sim C_{DNA}{}^{-2.4}$, as shown in Figure 18. For synthetic

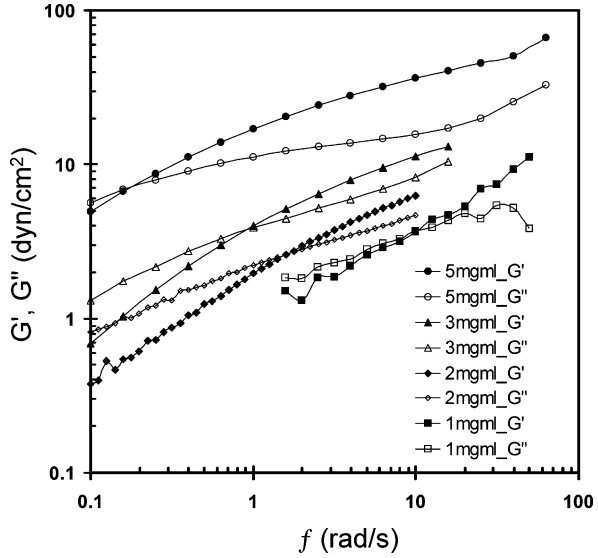

Figure 17. Storage and loss modulus in the frequency domain for the aqueous solutions of calf thymus DNA with concentration as a parameter measured at 293 K. Crossover frequency of G' and G'' shifts to lower frequency with an increasing concentration.

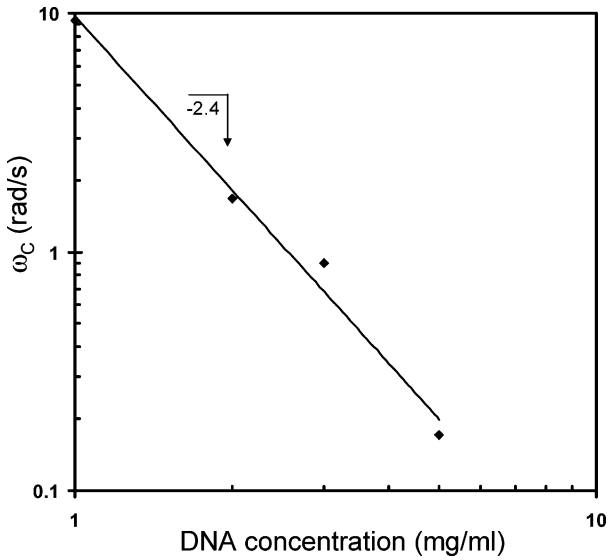

Figure 18. Crossover frequency of G' and G'' (ω_C) as a function of calf thymus DNA concentration. The scaling power is −2.4.

semiflexible polymers in a good solvent, there are two empirical correlations[26] that relate the plateau modulus and viscosity to concentration: $G'_p \sim C^{2.3}$ and $\eta \sim C^{4.7}$. The plateau storage modulus and viscosity are also related by[26] $G'_p = \eta\omega_C$, resulting in the crossover frequency scaling with concentration as $\omega_C \sim C_{DNA}{}^{-2.4}$—in excellent agreement with our experimental data. The implication is that the DNA molecules behave as semiflexible polymers in aqueous solution.[26]

Storage and loss modulus of a 5 mg/mL calf thymus DNA solution with temperature as a parameter (between 283 and 343 K) are plotted in Figure 19. A vertical shift of curves at different temperatures was employed for clarity. Similar results were obtained for the concentrations of 2 and 3 mg/mL; however, measurements at higher temperature for lower concentration were difficult due to low viscosity. It is clear that the crossover frequency shifts to higher frequency with increasing temperature. The relaxation time obtained

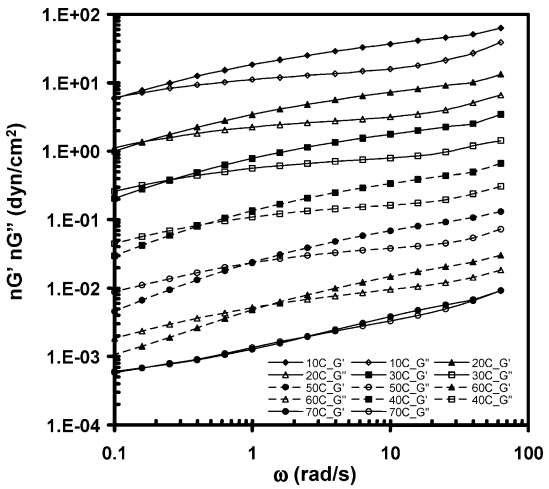

Figure 19. Storage and loss modulus for the aqueous solutions of calf thymus DNA in the frequency domain with temperature as a parameter during heating from 283 to 343 K. A vertical shift was employed for clarity.

from $\tau = 1/\omega_C$ has an Arrhenius-like temperature dependence. The calculated activation energy is 32 kJ/mol for all three concentrations; however a deviation from the Arrhenius behavior occurs above 50 °C. The DMS spectra show a noticeable difference below and above 50 °C, and the storage modulus starts to decrease considerably at a critical temperature of 50 °C. It appears that the rigid-rod-like DNA molecule in solution has lost its rigidity as a whole, possibly due to some "weak points" where the A−T pairs open up along the DNA molecules. This suggests that the DNA dynamics as measured by DMS are affected by the breakup of base pairs at temperature as low as 50 °C, well below the chain melting temperature (T_m = 87 °C) of the calf thymus DNA.

Conclusions

We have completed a comprehensive investigation of the dynamics of aqueous solutions of deoxyribonucleic acid (DNA) by DRS and DMS. Experimental results were generated over a wide rage of temperature and frequency, and the following principal conclusions are drawn.

Two relaxation processes are observed in the aqueous solutions of DNA at low temperature, and both obey the Arrhenius equation. The slower (lower frequency) process has a symmetric, Cole−Cole type spectrum and the activation energy of 55 kJ/mol. This process originates in the relaxation of ice within the ice−DNA matrix. The faster (higher frequency process) is Debye-like, has an activation energy of 27 kJ/mol, and is related to the bound water in the immediate vicinity of the DNA molecules. The average relaxation time for these processes is unaffected by the change in DNA concentration, and their molecular origin is corroborated by the observed trend in dielectric strength. The denatured DNA solution shows only one process at 203 K, with a shorter relaxation time (higher frequency) than that of the bound water in the native DNA. This is in agreement with Mashimo et al.,[7] who argued that bound water forms highly ordered clusters along and across the grooves of DNA, while the clusters are less ordered in the random coil state. A comparison of relaxation spectra of aqueous and water/glycerol solutions of DNA revealed that the DNA dynamics are dominated by the solvent. Interestingly, Caliskan et al.[42] have reached the same conclusion in their study of proteins in different solvents.

In the higher temperature range, encompassing the physiological condition, conductivity dominates the dielectric response. A pronounced peak in the dielectric modulus spectrum is observed, and its molecular origin is found to lie in the migration of counterions along the DNA surface. The observed decrease in the average relaxation time (τ) and increase in dielectric strength ($\Delta\epsilon$) with increasing DNA concentration are in agreement with the findings of Bone et al.[24] The average characteristic time obtained from the frequency of the dielectric loss modulus peak has the signature of a thermally activated process with an apparent activation energy of 30 kJ/mol. Using Manning's model, it was calculated that the subunit length over which counterions fluctuate increases from 70 nm at a concentration of 2 mg/mL to 153 nm at a concentration of 0.125 mg/mL.

The results of DMS measurements of aqueous solutions of calf thymus DNA reveal a *G′/G″* crossover point whose frequency (ω_C) scales with concentration as $\omega_C \sim C_{DNA}^{-2.4}$. The implication is that the DNA molecules behave as semiflexible polymers in aqueous solution. The temperature dependence of ω_C indicates that the breakup of the DNA base pairs and the chain melting begin at a temperature as low as 50 °C.

Acknowledgment. This material is based on work supported by National Science Foundation under Grants DMR-0101182 and DMR-9975592 (instrumentation grant). The authors are grateful to Dr. James Baker-Jarvis (NIST, Boulder, CO) for help with high-frequency measurements and Dr. Sridhar Venkataraman (Polytechnic) for help with DNA characterization.

References and Notes

(1) Moran, L. A.; Scimgeour, K. G.; Horton, H. R.; Ochs, R. S.; Rawn, J. D. *Biochemistry*, 2nd ed.; Neil Patterson Publishers: Prentice Hall, 1994.
(2) Manning, G. S. *Q. Rev. Biophys.* **1978**, *2*, 179.
(3) Baker-Jarvis, J.; Jones, C. A.; Riddle, B. *NIST Tech. Note* **1998**, *1509*.
(4) Takashima, S. *Electrical Properties of Biopolymers and Membranes*; Adam Hilger: Bristol, 1989.
(5) Pethig, R. *Dielectric and Electronic Properties of Biological Materials*; John Wiley & Sons: London, 1978.
(6) Watson, J. D.; Crick, F. H. *Nature (London)* **1953**, *171*, 737.
(7) Mashimo, S.; Umehara, T.; Kuwabara, S.; Yagihara, S. *J. Phys. Chem.* **1989**, *93*, 4963.
(8) Hayashi, Y.; Shinyashiki, N.; Yagihara, S.; Yoshiba, K.; Teramoto, A.; Nakamura, N.; Miyazaki, Y.; Sorai, M.; Wang, Q. *Biopolymers* **2002**, *63*, 21.
(9) Harvey, S. C.; Hoekstra, P. *J. Phys. Chem.* **1972**, *76*, 2987.
(10) Hayakawa, R.; Kanda, H.; Sakamoto, M.; Wada, Y. *Japan. J. Appl. Phys.* **1975**, *14*, 2039.
(11) Takashima, S.; Gabriel, C.; Sheppard, R. J.; Grant, E. H. *Biophys. J.* **1984**, *46*, 29.
(12) Foster, K. R.; Stuchly, M. A.; Kraszewski, A.; Stuchly, S. S. *Biopolymers* **1984**, *23*, 593.
(13) Mashimo, S.; Umehara, T.; Ota, T.; Kuwabara, S.; Shinayashiki, N.; Yagihara, S. *J. Mol. Liq.* **1987**, *36*, 135.
(14) Nandi, N.; Bagchi, B. *J. Phys. Chem. B* **1997**, *101*, 10954.
(15) Nandi, N.; Bhattacharyya, K.; Bagchi, B. *Chem. Rev.* **2000**, *100*, 2013.
(16) Takashima, S. *J. Phys. Chem.* **1966**, *70*, 1372.
(17) Allgen, L. G. *Acta Physiol. Scand. Suppl.* **1950**, *22*, 32.
(18) Mandel, M. *Ann. N.Y. Acad. Sci.* **1977**, *303*, 74.
(19) Vreugdenhil, T.; Touw, F. V. d.; Mandel, M. *Biophys. Chem.* **1979**, *10*, 67.
(20) Grosse, C. *Alta Frequenza* **1989**, *58*, 365.
(21) Pedone, F.; Bonincontro, A. *Biochim. Biophys. Acta* **1991**, *1073*, 580.

(22) Bonincontro, A.; Matzeu, M.; Mazzei, F.; Minoprio, A.; Pedone, F. *Biochim. Biophys. Acta* **1993**, *1171*, 288.
(23) Saif, B.; Mohr, R. K.; Montrose, C. I.; Litovitz, T. A. *Biopolymers* **1991**, *31*, 1171.
(24) Bone, S.; Small, C. A. *Biochim. Biophys. Acta* **1995**, *1260*, 85.
(25) Bone, S.; Lee, R. S.; Hodgson, C. E. *Biochim. Biophys. Acta* **1996**, *1306*, 93.
(26) Mason, T. G.; Dhople, A.; Wirtz, D. *Macromolecules* **1998**, *31*, 3600.
(27) Mason, T. G.; Dhople, A.; Wirtz, D. *Mater. Res. Soc. Symp. Proc.* **1997**, *463*, 153.
(28) Mason, T. G.; Weitz, D. A. *Phys. Rev. Lett.* **1995**, *74*, 1250.
(29) Mason, T. G.; Ganesan, K.; Zanten, J. H. v.; Wirtz, D.; Kuo, S. C. *Phys. Rev. Lett.* **1997**, *79*, 3282.
(30) Mason, T. G. *Rheol. Acta* **2000**, *39*, 371.
(31) Schmidt, F. G.; Hinner, B.; Sackmann, E. *Phys. Rev. E.* **2000**, *61*, 5646.
(32) Chen, D. T.; Weeks, E. R.; Crocker, J. C.; Islam, M. F.; Verma, R.; Gruber, J.; Levine, A. J.; Lubensky, T. C.; Yodh, A. G. *Phys. Rev. Lett.* **2003**, *90*, 108301.
(33) Cheng, Z.; Mason, T. G. *Phys. Rev. Lett.* **2003**, *90*, 018304.
(34) Gardel, M. L.; Valentine, M. T.; Crocker, J. C.; Bausch, A. R.; Weitz, D. A. *Phys. Rev. Lett.* **2003**, *91*, 158302.
(35) Lau, A. W. C.; Hoffman, B. D.; Davies, A.; Crocker, J. C.; Lubensky, T. C. *Phys. Rev. Lett.* **2003**, *91*, 198101.
(36) Suherman, P. M.; Taylor, P.; Smith, G. *J. Non-Cryst. Solids* **2002**, *305*, 317.
(37) Havriliak, S. J.; Negami, S. *Polymer* **1967**, *8*, 161.
(38) Cole, R. H.; Cole, K. S. *J. Chem. Phys.* **1942**, *10*, 98.
(39) Miura, N.; Hayashi, Y.; Mashimo, S. *Biopolymers* **1996**, *39*, 183.
(40) Auty, R. P.; Cole, R. H. *J. Chem. Phys.* **1952**, *20*, 1309.
(41) Sudo, S.; Shimomura, M.; Shinyashiki, N.; Yagihara, S. *J. Non-Cryst. Solids* **2002**, *307*−*310*, 356.
(42) Caliskan, G.; Mechtani, D.; Roh, J. H.; Kisliuk, A.; Sokolov, A. P.; Azzam, S.; Peral, I. *J. Chem. Phys.* **2004**, *121*, 1978.
(43) Samouillan, V.; Lamure, A.; Lacabanne, C. *Chem. Phys.* **2000**, *255*, 259.
(44) Roling, B. *Dielectrics Newsletter* **2002**, *Nov*, 1.
(45) Moznine, R. E.; Smith, G.; Polygalov, E.; Suherman, P. M.; Broadhead, J. *J. Phys. D: Appl. Phys.* **2003**, *36*, 330.
(46) Richert, R.; Wagner, H. *Solid State Ionics* **1998**, *105*, 167.
(47) Macdonald, J. R. *Impedance Spectroscopy: Emphasizing Solid Materials and Systems*; John Wiley & Sons: New York, 1987.
(48) Hasz, W. C.; Moynihan, C. T.; Tick, P. A. *J. Non-Cryst. Solids* **1994**, *172*−*174*, 1363.
(49) Moynihan, C. T. *J. Non-Cryst. Solids* **1996**, *203*, 359.
(50) Ngai, K. L.; Moynihan, C. T. *MRS Bull.* **1998**, *23*, 51.
(51) Moynihan, C. T. *Solid State Ionics* **1998**, *105*, 175.
(52) Parthum, M. G.; Johari, G. P. *J. Chem. Soc., Faraday Trans.* **1995**, *91*, 329.
(53) Wagner, H.; Richert, R. *Polymer* **1997**, *38*, 255.
(54) Bonincontro, A.; De Francesco, A.; Onori, G. *Colloids Surf., B* **1998**, *12*, 1.
(55) Grant, E. H.; Sheppard, R. J.; South, G. P. *Dielectric Behaviour of Biological Molecules in Solution*; Clarendon: Oxford, 1978.
(56) Touw, F. v. d.; Mandel, M. *Biophys. Chem.* **1974**, *2*, 218.
(57) Touw, F. v. d.; Mandel, M. *Biophys. Chem.* **1974**, *2*, 231.
(58) Manning, G. S. *J. Chem. Phys.* **1969**, *51*, 924.
(59) Penafiel, L. M.; Litovitz, T. A. *J. Chem. Phys.* **1992**, *97*, 559.
(60) Georgakilas, A. G.; Haveles, K. S.; Sideris, E. G. *IEEE Trans. Dielectr. Electr. Insul.* **1998**, *5*, 26.
(61) (a) Vogel, H. *Phys. Z.* **1921**, *22*, 645. (b) Fulcher, G. S. *J. Am. Ceram. Soc.* **1923**, *8*, 339. (c) Tammann, G.; Hesse. W. Z. *Anorg. Allg. Chem.* **1926**, *156*, 245.

MA051596J